Antibacterial Balsacones J–M, Hydroxycinnamoylated Dihydrochalcones from Populus balsamifera Buds

ARTICLE *in* JOURNAL OF NATURAL PRODUCTS · APRIL 2015

Impact Factor: 3.8 · DOI: 10.1021/acs.jnatprod.5b00155 · Source: PubMed

JOURNAL OF NATURAL PRODUCTS

Article

pubs.acs.org/jnp

Antibacterial Balsacones J–M, Hydroxycinnamoylated Dihydrochalcones from *Populus balsamifera* Buds

François Simard,[†] Charles Gauthier,[†,‡] Éric Chiasson,[†] Serge Lavoie,[†] Vakhtang Mshvildadze,[†] Jean Legault,[†] and André Pichette*[,†]

[†]Chaire de Recherche sur les Agents Anticancéreux d'Origine Naturelle, Laboratoire LASEVE, Département des Sciences Fondamentales, Université du Québec à Chicoutimi, 555 Boulevard de l'Université, Chicoutimi, Québec, Canada, G7H 2B1

[‡]Institut de Chimie IC2MP, CNRS-UMR 7285, Équipe Synthèse Organique, Université de Poitiers, 4 Rue Michel Brunet, 86073 Poitiers Cedex-9, France

Supporting Information

ABSTRACT: A phytochemical investigation of buds from the hardwood tree *Populus balsamifera* led to the isolation of six new cinnamoylated dihydrochalcones as pairs of racemates and one as a racemic mixture along with the known compound iryantherin-D (**2**), the absolute configuration of which was determined for the first time. The structures of balsacones J (**1**), K (**3**), L (**4**), and M (**5**) were elucidated on the basis of spectroscopic data (1D and 2D NMR, IR, and MS). Chiral HPLC separations were carried out, and the absolute configuration of the isolated enantiomers unambiguously established via X-ray diffraction analyses and electron circular dichroism spectroscopic data. Each of the purified enantiomers exhibited potent in vitro antibacterial activity against *Staphylococcus aureus* with IC_{50} values ranging from 0.61 to 6 μM.

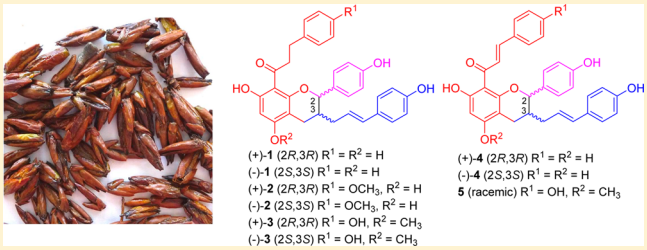

With the growth of antibiotic resistance in bacterial species, the need for new classes of antibacterial agents is becoming stronger.[1] Historically, microbial secondary metabolism has been the most abundant source of new antibiotic scaffolds. Despite this, only two new classes of antibiotics have reached the market in the last 50 years, prompting the exploration of alternative strategies.[2] Natural products from plants are considered to be a potential source of new antibiotic scaffolds.[3] Indeed, the use of plants to treat bacterial infections is already widespread in traditional medicine around the world.[4−8] Moreover, antibacterial properties have been shown both in vitro and in vivo for many plant-based natural products.[9,10]

Reports of the traditional medicines used by Canadian Aboriginals frequently mention the use of buds from *Populus balsamifera* L.[4] Treatments of dermatological and gastro-intestinal troubles are examples of their many traditional uses. Recently, our research group has undertaken the task of identifying the compounds implicated in the antibacterial activity of an ethanolic extract of *P. balsamifera* buds. This work resulted in the identification of new dihydrocinnamoyl flavans and hydroxycinnamoylated dihydrochalcones exhibiting potent in vitro antibacterial activities against *Staphylococcus aureus*.[11,12] In the present study, further investigation of an ethanolic extract of *P. balsamifera* buds led to the isolation of eight hydroxycinnamoylated dihydrochalcones as pairs of racemates (**1**−**4**) and one as a racemic mixture (**5**). Their structures were elucidated based upon the analysis of spectroscopic data, and their absolute configurations established with the help of X-ray single-crystal diffraction analysis and electron circular dichroism (ECD) data. The antibacterial activity and cytotoxicity of all purified enantiomers and racemic mixtures were evaluated in vitro against *S. aureus* and human skin fibroblast cells (WS1), respectively.

RESULTS AND DISCUSSION

Fractionation of an ethanolic extract of *P. balsamifera* buds by liquid−liquid extraction, silica gel, and reversed-phase column chromatography, followed by preparative HPLC purification, afforded compounds **1**−**5**.

Balsacone J (**1**) was obtained as a yellow powder. Its molecular formula was established as $C_{33}H_{30}O_6$ (19 indices of hydrogen deficiency) based on the $[M + Na]^+$ quasi-molecular ion peak at 545.1945 (calcd 545.1935) in the HRMS spectrum and ^{13}C NMR spectroscopic data. The IR spectrum of **1** showed bands at 3352 cm^{-1} (phenol) and 1612 cm^{-1} (carbonyl). The ^1H and ^{13}C NMR data (Tables 1 and 2, respectively) combined with information from DEPT135 and HSQC spectra suggested the presence of one carbonyl, five oxygenated aromatic quaternary carbons, five aromatic carbons, nine sp^2 methines, two sp^3 methines (one oxygenated), and four methylenes, indicating that some of these signals represented equivalent carbons. Analysis of 1D ^1H, 2D-COSY, and HSQC experiments (Figure 1) showed signals for two 1,4-disubstituted aromatic rings at δ_H 6.92 (2H, d, 8.5 Hz,

Received: February 13, 2015
Published: April 30, 2015

DOI: 10.1021/acs.jnatprod.5b00155
J. Nat. Prod. 2015, 78, 1147−1153

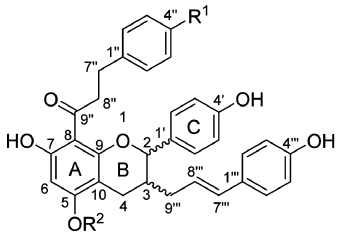

(+)-**1** (2*R*,3*R*) $R^1 = R^2 = H$
(-)-**1** (2*S*,3*S*) $R^1 = R^2 = H$
(+)-**2** (2*R*,3*R*) $R^1 = OCH_3$, $R^2 = H$
(-)-**2** (2*S*,3*S*) $R^1 = OCH_3$, $R^2 = H$
(+)-**3** (2*R*,3*R*) $R^1 = OH$, $R^2 = CH_3$
(-)-**3** (2*S*,3*S*) $R^1 = OH$, $R^2 = CH_3$

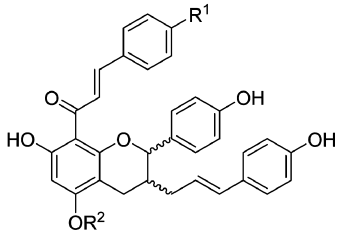

(+)-**4** (2*R*,3*R*) $R^1 = R^2 = H$
(-)-**4** (2*S*,3*S*) $R^1 = R^2 = H$
5 (racemic) $R^1 = OH$, $R^2 = CH_3$

Table 1. ^{1}H NMR Spectroscopic Data for Compounds 1−5 in Acetone-d_6 (400 MHz)

	δ_H (J in Hz)				
position	1	2	3	4	5
2	4.85, d (9.4)	4.85, d (9.3)	4.79, d (9.3)	4.85, d (9.4)	4.81, d (9.8)
3	2.29, m	2.26, m	2.24, m	2.23, m	2.36, m
4_{ax}	2.40, dd (16.2, 11.2)	2.30, dd (16.1, 10.9)	2.31, dd (16.1, 11.1)	2.41, m	2.34, m
4_{eq}	2.91, dd (16.2, 5.0)	2.91, dd (16.1, 4.6)	2.83, dd (16.1, 4.2)	2.98, m	2.91, m
6	6.02, s	6.02, s	6.08, s	6.07, s	6.10, s
2′/6′	7.39, d (8.5)	7.41, d (8.4)	7.38, d (8.2)	7.53, d (8.4)	7.50, d (8.4)
3′/5′	6.92, d (8.5)	6.94, d (8.4)	6.94, d (8.2)	7.04, d (8.4)	7.04, d (8.4)
2″/6″	6.83, d (7.1)	6.71, s	6.62, s	7.06, d (8.1)	6.96, d (8.6)
3″/5″	7.15, t (7.1)	6.71, s	6.62, s	7.26, m	6.78, m
4″	7.08, t (7.1)			7.29, m	
7″	2.82, dd (9.2, 7.7)	2.74, dd (9.5, 7.7)	2.71, dd (9.3, 7.6)	7.61, d (15.7)	7.61, d (15.5)
8″	3.17, m	3.12, m	3.12, m	8.04, d (15.7)	7.92, d (15.5)
2‴/6‴	7.23, d (8.6)	7.23, d (8.5)	7.22, d (8.2)	7.25, d (8.5)	7.26, d (8.6)
3‴/5‴	6.77, d (8.6)	6.77, d (8.5)	6.77, d (8.2)	6.77, d (8.5)	6.78, m
7‴	6.32, d (16.0)	6.31, d (15.7)	6.30, d (15.7)	6.33, d (15.8)	6.33, d (15.8)
8‴	6.04, m	6.05, m	6.03, m	6.05, m	6.07, m
9‴a	2.02, m	2.00, m	1.97, m	2.02, m	2.01, m
9‴b	2.19, m	2.19, m	2.17, m	2.23, m	2.22, m
7-OH	13.78, s	13.82, s	13.95, s	14.46, s	
4″-OCH_3		3.74, s			
5-OCH_3			3.83, s		3.88, s

H-3′/5′), 7.39 (2H, d, 8.5 Hz, H-2′/6′), 6.77 (2H, d, 8.6 Hz, H-3‴/5‴), and 7.23 (2H, d, 8.6 Hz, H-2‴/6‴) and one monosubstituted aromatic ring at δ_H 6.83 (2H, d, 7.1 Hz, H-2″/6″), 7.15 (2H, t, 7.1 Hz, H-3″/5″), and 7.08 (1H, t, 7.1 Hz, H-4″). In the COSY spectrum, another coupling system consisting of an sp^3 methine at δ_H 2.29 (1H, m, H-3) coupled to a diastereotopic methylene at δ_H 2.40 (1H, dd, 16.2 and 11.2 Hz, H-4_{ax}) and 2.91 (1H, dd, 16.2 and 5.0 Hz, H-4_{eq}) and to another sp^3 methine at δ_H 4.85 (1H, d, 9.4 Hz, H-2) was reminiscent of the C-ring signals of a flavan skeleton. Indeed, HMBC correlations of H-2′/6′ with C-2 (δ_C 84.2) and C-4′ (δ_C 158.6) showed that one of the 1,4-disubstituted aromatic rings was oxygenated and linked to C-2, thereby forming the B-ring of the flavan skeleton. The presence of a hydrogen-bonded phenolic hydrogen atom was detected based on the signal at δ_H 13.78 (1H, s, 7-OH). Its HMBC correlations with C-6 (δ_C 96.2), C-7 (δ_C 166.0), and C-8 (δ_C 105.5) suggested it was situated on the A-ring of the flavan skeleton. The hydrogen bond of the phenolic hydrogen was further supported by additional weak HMBC correlations of 7-OH with C-9″ (δ_C 205.3) and C-5 (δ_C 163.2). The latter ^4J correlation could be explained by a *W*-configuration. Assignments of other signals associated with the A-ring were deduced from the following HMBC correlations (Figure 1): H-6 (δ_H 6.02, 1H, s), H-4_{ax}, and H-4_{eq} with C-5; H-6 with C-7, C-8, and C-10 (δ_C 102.2); H-4_{ax} and H4_{eq} with C-9 (δ_C 159.3). Another coupling system detected on the COSY spectrum consisted of two methylenes at δ_H 2.82 (2H, dd, 9.2 and 7.7 Hz, H-7″) and 3.17 (2H, m, H-8″). The HMBC correlations of H-7″ and H-8″ with C-9″ (δ_C 205.3) and of H-2″/6″ with C-7″ (δ_C 31.1) suggested that the two methylenes were linked to a carbonyl and to the monosubstituted aromatic ring, resulting in a dihydrocinnamoyl unit. A *W*-coupling between H-6 and C-9″ observed in the HMBC spectrum indicated that the dihydrocinnamoyl unit was attached to ring A. Also, the APCI(+)MS fragment of m/z 271 corresponding to the typical retro Diels−Alder fragment of flavonoids[13] was present (Figure 1). With only positions 6 and 8 available, it was determined that the dihydrocinnamoyl unit was at C-8 based on the 2D NOESY correlations of H-8″ with H-2 and H-2′/6′. The remaining signals comprised an allyl moiety at δ_H 6.32 (1H, d, 16.0 Hz, H-7‴), 6.04 (1H, m, H-8‴), 2.02 (1H, m, H-9‴a), and 2.19 (1H, m, H-9‴b) and the second 1,4-disubstituted aromatic ring. The HMBC correlations of H-2‴/6‴ with C-7‴ (δ_C 132.6) and C-4‴ (δ_C 157.6) indicated that the 1,4-disubstituted aromatic ring was oxygenated and linked to the allyl group, resulting in a 4-hydroxycinnamoyl unit. The only available position for this unit was at C-3, which was confirmed by the HMBC correlation of H-4_{ax} with C-9‴ (δ_C 36.2). On the basis of the above evidence, balsacone J (**1**) was characterized as 1-[3-[(*E*)-1-(4-hydroxyphenyl)propen-3-yl]-3,4-dihydro-5,7-dihydroxy-2-(4-hydroxyphenyl)-2*H*-chromen-8-yl]-3-phenylpropan-1-one.

Balsacone K (**3**) was obtained as a yellow powder. Its molecular formula was established as $C_{34}H_{32}O_7$ (19 indices of hydrogen deficiency) based on the $[M + Na]^+$ quasi-molecular ion at 575.2042 (calcd 575.2040) in the HRMS spectrum and ^{13}C NMR spectroscopic data. The NMR spectroscopic data of **3** (Tables 1 and 2) were similar to those of **1**. The first difference observed was the presence of an additional methoxy signal (5-OCH_3) at δ_H 3.83 (3H, s) and δ_C 56.2. The position of the methoxy group was established as C-5 based on the HMBC correlation of the methoxy protons with C-5 (δ_C 164.5). The second difference was a change in the chemical shifts for the protons and carbons of the aromatic linked to the methylene at C-7″. This change was attributed to the presence of a hydroxy group at C-4″, as shown by its chemical shift at δ_C

DOI: 10.1021/acs.jnatprod.5b00155
J. Nat. Prod. 2015, 78, 1147−1153

Table 2. ^{13}C NMR of Compounds 1−5 in Acetone-d_6 (100 MHz)

	δ_C, type				
position	1	2	3	4	5
2	84.2, CH	84.1, CH	84.0, CH	84.4, CH	84.3, CH
3	37.8, CH	37.7, CH	37.7, CH	37.4, CH	37.3, CH
4	26.0, CH_2	26.0, CH_2	26.0, CH_2	26.4, CH_2	26.4, CH_2
5	163.2, C	163.2, C	164.5, C	163.7, C	164.7, C
6	96.2, CH	96.2, CH	92.8, CH	96.4, CH	93.1, CH
7	166.0, C	166.0, C	166.5, C	167.4, C	168.0, C
8	105.5, C	105.4, C	105.8, C	105.7, C	105.9, C
9	159.3, C	159.3, C	158.2, C	159.2, C	158.1, C
10	102.2, C	102.2, C	102.8, C	102.6, C	103.4, C
1′	131.0, C	131.1, C	130.9, C	131.0, C	130.9, C
2′/6′	129.8, CH	129.9, CH	129.8, CH	130.4, CH	130.4, CH
3′/5′	116.3, CH	116.4, CH	116.4, CH	116.6, CH	116.6, CH
4′	158.6, C	158.7, C	158.7, C	158.9, C	158.9, C
1″	142.2, C	133.9, C	132.6, C	136.3, C	127.9, C
2″/6″	129.0, CH	129.8, CH	129.8, CH	129.1, CH	131.2, CH
3″/5″	129.0, CH	114.3, CH	115.8, CH	129.6, CH	116.6, CH
4″	126.3, CH	158.7, C	156.1, C	130.6, CH	160.5, C
7″	31.1, CH_2	29.9, CH_2	30.3, CH_2	142.6, CH	143.7, CH
8″	45.7, CH_2	46.0, CH_2	46.1, CH_2	128.6, CH	125.2, CH
9″	205.3, C	205.4, C	205.9, C	192.9, C	193.2, C
1‴	132.6, C	130.1, C	130.1, C	130.1, C	130.1, C
2‴/6‴	128.2, CH	128.2, CH	128.1, CH	128.2, CH	128.2, CH
3‴/5‴	116.1, CH	116.1, CH	116.2, CH	116.1, CH	116.2, CH
4‴	157.6, C	157.6, C	157.6, C	157.6, C	157.6, C
7‴	132.6, CH	132.6, CH	132.6, CH	132.7, CH	132.7, CH
8‴	124.5, CH	124.5, CH	124.5, CH	124.4, CH	124.4, CH
9‴	36.2, CH_2	36.2, CH_2	36.2, CH_2	36.2, CH_2	36.2, CH_2
5-OCH_3			56.2, CH_3		26.3, CH_3
4″-OCH_3		55.3, CH_3			

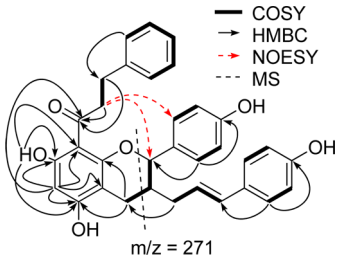

Figure 1. HMBC, COSY, NOESY, and MS data for identification of balsacone J (**1**).

156.1. Since the molecular formula established for **3** accounted for only one more oxygen, it was considered to be a phenolic function, thus indicating that **3** possessed a 4-hydroxydihydrocinnamoyl unit. This unit was determined to be at C-8 using the 2D NOESY correlations of H-8″ (δ_H 3.12, 2H, m) with H-2 (δ_H 4.79, 1H, d, 9.3 Hz) and H-2′/6′ (δ_H 7.38, 2H, d, 8.2 Hz). On the basis of the above evidence, balsacone K (**3**) was characterized as 1-[3-[(*E*)-1-(4-hydroxyphenyl)propen-3-yl]-3,4-dihydro-7-hydroxy-5-methoxy-2-(4-hydroxyphenyl)-2*H*-chromen-8-yl]-3-(4-hydroxyphenyl)propan-1-one.

Balsacone L (**4**) was obtained as a yellow powder. Its molecular formula was established as $C_{33}H_{28}O_6$ based on the ^{13}C NMR spectroscopic data and an $[M + Na]^+$ quasi-molecular ion peak at 543.1781 (calcd 543.1778) in the HRMS spectrum. The NMR spectroscopic data of **4** (Tables 1 and 2) were similar to those of **1** except for the dihydrocinnamoyl unit. HMBC correlations of H-7″ (δ_H 7.61, 1H, d, 15.7 Hz) and H-8″ (δ_H 8.04, 1H, d, 15.7 Hz) with C-9″ (δ_C 192.9) suggested the presence of an enone moiety. Furthermore, HMBC correlations of H-2″/6″ (δ_H 7.06, 2H, d, 8.1 Hz) with C-7″ (δ_C 142.6) showed that the enone unit was conjugated with a monosubstituted aromatic ring, resulting in a cinnamoyl unit. The position of the cinnamoyl group was determined to be at C-8 based on the NOESY correlation of H-8″ with H-2 (δ_H 4.85, 1H, d, 9.4 Hz). On the basis of the above evidence, balsacone L (**4**) was characterized as 1-[3-[(*E*)-1-(4-hydroxyphenyl)propen-3-yl]-3,4-dihydro-5,7-dihydroxy-2-(4-hydroxyphenyl)-2*H*-chromen-8-yl]-3-phenylprop-2-en-1-one.

Balsacone M (**5**) was obtained as a yellow powder. Its molecular formula was established as $C_{34}H_{30}O_7$ based on the ^{13}C NMR spectroscopic data and an $[M + Na]^+$ quasi-molecular ion peak at 573.1871 (calcd 573.1884) in the HRMS spectrum. The NMR spectroscopic data of **5** (Tables 1 and 2) were similar to those of **4**. The discrepancies between the two were attributed to the presence of a methoxy group at C-5 and a hydroxy group at C-4″ in compound **5**. The position of the methoxy group was determined based on the HMBC correlation of 5-OCH_3 (δ_H 3.88) with C-5 (δ_C 164.7). The additional hydroxyl group was deduced from the 1,4-disubstituted pattern of H-2″/6″ and H-3″/5″, the chemical shift of C-4″ (δ_C 160.5), and the additional oxygen in the molecular formula. The position of the 4-hydroxycinnamoyl group was determined to be at C-8 based on the NOESY correlation of H-8″ (δ_H 7.92, 1H, d, 15.5 Hz) with H-2 (δ_H 4.81, d, 9.8 Hz). On the basis of the above evidence, balsacone M (**5**) was characterized as 1-[3-[(*E*)-1-(4-hydroxyphenyl)-

DOI: 10.1021/acs.jnatprod.5b00155
J. Nat. Prod. 2015, 78, 1147−1153

propen-3-yl]-3,4-dihydro-7-hydroxy-5-methoxy-2-(4-hydroxyphenyl)-2*H*-chromen-8-yl]-3-(4-hydroxyphenyl)prop-2-en-1-one.

Compound **2** was previously reported as iryantherin-D in a phytochemical investigation of *Iryanthera laevis* Markgr. (Myristicaceae).[14] Spectroscopic data for **2** (^{1}H, ^{13}C, UV, and IR) were in good agreement with those of iryantherin-D. The absolute configuration of iryantherin-D (**2**) was not determined previously; therefore this task was undertaken in this study along with the determination of the absolute configuration of the other isolated compounds (**1**, **3**, **4**).

The relative configuration of all isolated compounds was established as 2,3-*trans* based on $J_{2,3}$ coupling constants ranging from 9.3 to 9.8 Hz. Measurement of the optical rotations of compounds **1**−**5** gave $[\alpha]_D$ values of 0. Moreover, no Cotton effects were observed in their ECD spectra, suggesting that they were racemic mixtures. Chiral analytical HPLC analysis of all isolated compounds confirmed the presence of two enantiomers in equal amounts. Chiral semipreparative HPLC purifications were undertaken for compounds **1**−**4**, yielding (+)-balsacone J [(+)-**1**], (−)-balsacone J [(−)-**1**], (+)-iryantherin-D [(+)-**2**], (−)-iryantherin-D [(−)-**2**], (+)-balsacone K [(+)-**3**], (−)-balsacone K [(−)-**3**], (+)-balsacone L [(+)-**4**], and (−)-balsacone L [(−)-**4**]. Balsacone M (**5**) was not available in sufficient quantities (<9 mg) for further chiral purification. Crystals of (−)-**1** were obtained after recrystallization from isopropyl alcohol (IPA), and its absolute configuration was determined to be (2*S*,3*S*) from single-crystal X-ray diffraction analysis using direct methods (Figure 2).

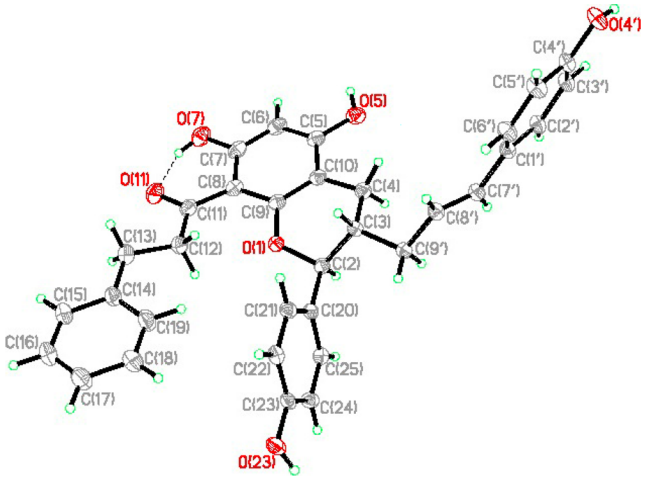

Figure 2. Single-crystal X-ray structure of (−)-**1**.

Computational calculations of ECD spectra of the (2*S*,3*S*)-enantiomers of compounds **1**−**4** were also performed using time-dependent density functional theory (TDDFT). Comparison of these calculated spectra with experimental ECD spectra obtained from the isolated enantiomers allowed us to determine their absolute configuration (Figure 3). Experimental ECD spectra of (−)-**1**, (−)-**2**, and (−)-**3** all revealed two positive Cotton effects (CEs) around 225 and 260 nm and two negative CEs around 240 and 285 nm, which were in good agreement with the calculated ECD spectra indicating a (2*S*,3*S*) absolute configuration (Figure 3). X-ray diffraction and ECD calculation results were in agreement with the (2*S*,3*S*) absolute configuration for (−)-**1**. Experimental ECD spectra of (+)-**1**, (+)-**2**, and (+)-**3** were mirror images relative to those of their respective (−)-enantiomers and were therefore assigned (2*R*,3*R*) absolute configurations. Regarding balsacone M, the experimental ECD spectrum of (−)-**4** showed two positive CEs at 224 and 260 nm and two negative CEs at 233 and 286 nm, while that of (+)-**4** was its mirror image (Figure 3). The pattern obtained for calculated ECD spectra of (2*S*,3*S*)-**4** was similar to that of (−)-**4**. Therefore, the absolute configurations of (−)-**4** and (+)-**4** were determined to be (2*S*,3*S*) and (2*R*,3*R*), respectively.

A plausible biosynthetic pathway for compounds **1**−**5** is proposed in Figure 4. The previously isolated dihydrochalcones **6**−**8**[12] are likely to be precursors of isolated compounds **1**−**5**. Hydroxycinnamoylation of dihydrochalcones **6**−**8** at C-10 would generate compounds **9**−**11**, which would undergo a nonstereospecific 1,4-Michael addition, leading to the formation of the B-ring of flavanones **12**−**14** (enol form). Thereafter, an additional *trans*-hydroxycinnamoylation at C-3 would give derivatives **15**−**17**. Reduction of the latter compounds at both C-9‴ and C-4 positions would explain the formation of isolates **1**, **3**, and **2**, respectively. Another possible biosynthetic pathway would involve the reduction of the "keto" form of compounds **12**−**14** followed by a *trans*-hydroxycinnamoylation at C-3 and a reduction at C-9‴, which would generate isolates **1**−**3**. The formation of the remaining isolates **4** and **5** would be possible owing to the dehydrogenation at C-7″/8″ of compounds **1** and **3**, respectively.

The antibacterial activity of isolated enantiomers **1**−**4**, as well as racemic **5**, were evaluated in vitro against *S. aureus* after 24 h of incubation. The results presented in Table 3 are expressed as the concentrations inhibiting 50% of the bacterial growth (IC_{50}). Chloramphenicol and gentamycin were used as positive controls, with IC_{50} values of 0.43 and 0.010 μM, respectively. All compounds (**1**−**5**) demonstrated in vitro antibacterial activity against *S. aureus* with IC_{50} values ranging from 0.61 to 6 μM. Compound (−)-**4** was found significantly more active than the other compounds, with an IC_{50} value of 0.61 ± 0.02 μM. Interestingly, comparison of the IC_{50} values for each pair of enantiomers (**1**−**4**) showed that the (−)-enantiomers were significantly more active than the (+)-enantiomers. The isolated compounds were also evaluated for their cytotoxic activity against healthy cells (WS1) and found to be inactive (>10 μM). We recently showed that dihydrochalcones featuring an alkyl substituent on the A-ring may represent a promising chemical scaffold from which to generate new classes of antibiotic agents.[11,12] The results obtained in this study confirmed this hypothesis by revealing that derivatives bearing an additional hydroxycinnamoyl unit on the cyclized dihydrochalcone core also exhibited potent antibacterial activity.

EXPERIMENTAL SECTION

General Experimental Procedures. The melting point was measured on a Mettler Toledo MP70 melting point system (60−350 °C, 5 °C/min, uncorrected). Optical rotations were determined at the sodium D line (590 nm) on a Rudolph Research Analytical Autopol IV automatic polarimeter. UV spectra were recorded using an Agilent 8453 diode-array spectrophotometer. ECD spectra were recorded on a Jasco J-815 CD spectrometer. IR spectra were conducted on a PerkinElmer SpectrumOne (neat, thin films, on NaCl plates). ^{1}H, ^{13}C, and 2D NMR (^{1}H−^{1}H COSY, NOESY, HSQC, and HMBC) spectra were performed using an Avance 400 Bruker spectrometer (400.13 MHz for ^{1}H, 100.61 MHz for ^{13}C spectra) equipped with a 5 mm QNP probe in acetone-d_6. Chemical shift values were reported in ppm (δ) relative to TMS. High-resolution ESIMS spectra were obtained with an Agilent Technologies 6210 TOFMS system. Low-resolution

DOI: 10.1021/acs.jnatprod.5b00155
J. Nat. Prod. 2015, 78, 1147−1153

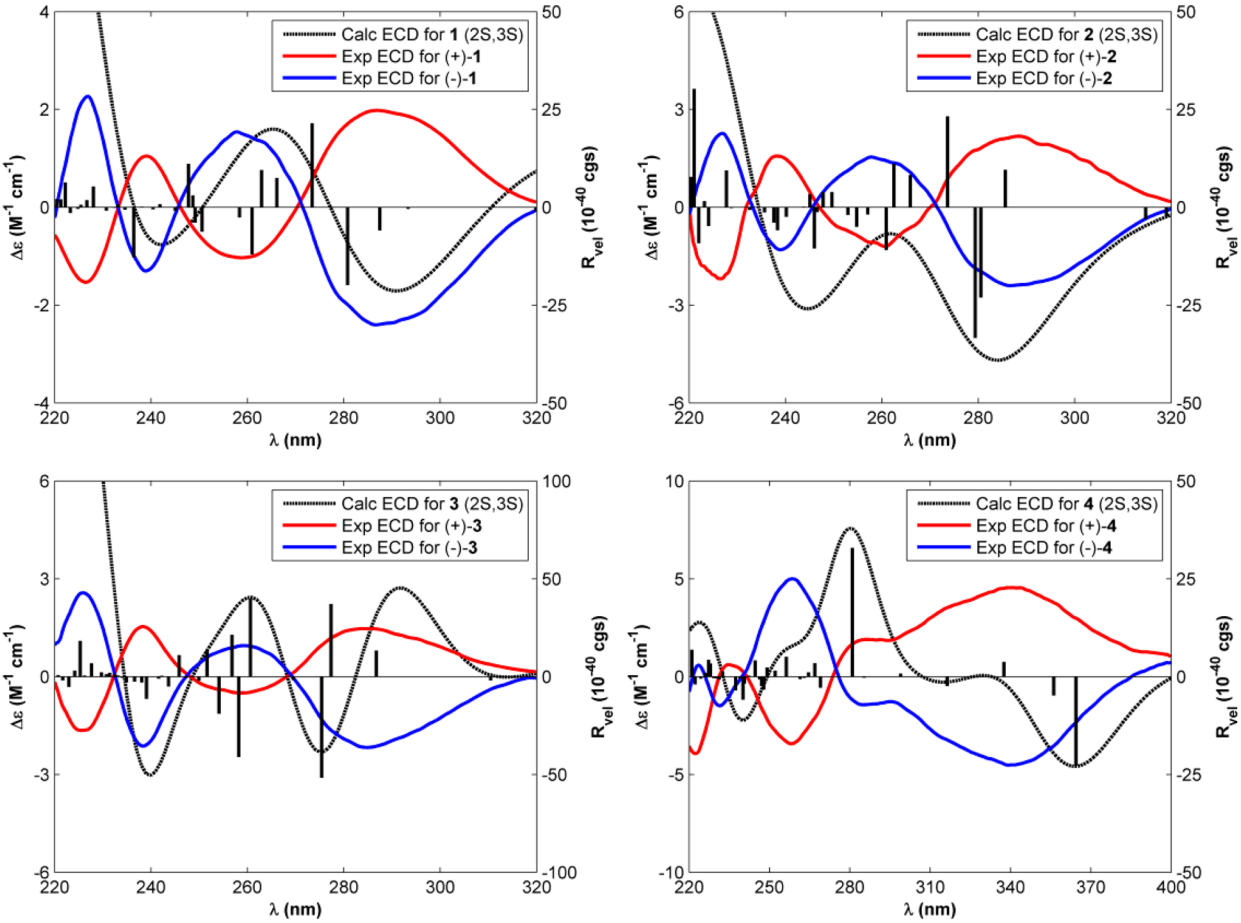

Figure 3. Experimental ECD spectra for compounds **1**−**4** overlaid with calculated (TDDFT at the B3LYP/6-311G(2d,2p) level) ECD spectra of compounds **1**-(2*S*,3*S*), **2**-(2*S*,3*S*), **3**-(2*S*,3*S*), and **4**-(2*S*,3*S*).

APCIMS (positive mode) were obtained with an Agilent G1946 VL mass selective detector. Column chromatography was performed using ultrapure silica gel (40−63 μm) supplied by Silicycle Inc. (Québec City, Canada). Reversed-phase flash chromatography was performed on a Biotage Flash+ system using a C_{18} 40iM cartridge (17%, 135 g) from Silicycle Inc. (Québec City, Canada). Semipreparative HPLC was carried out on an Agilent 1100 Series equipped with a UV−vis detector at 254 nm with an Inerstil Prep ODS column (20 × 250 mm, 10 μm) at a flow rate of 10 mL/min. Chiral semipreparative HPLC was conducted with the same instrument using a RegisPack chiral column (10.0 × 250 mm, 5 μm) at a flow rate of 4 mL/min. Reagents and analytical grade solvents were purchased from VWR International (Mont-Royal City, Canada) and were used as received.

Plant Material. Buds from different trees of *P. balsamifera* were collected in March 2005 near Chicoutimi (Québec), Canada. The plant was authenticated by Mr. Patrick Nadeau (Université du Québec à Chicoutimi), and a voucher specimen (No. 499678) was deposited at the Louis-Marie Herbarium of Université Laval, Québec City, Canada. After collection, buds were kept frozen until extraction.

Extraction and Isolation. Buds were ground and extracted as previously described.[11] The obtained residue was fractionated by liquid−liquid extraction and by three chromatography steps to afford five fractions (A−E).[11] Fraction B (6.3 g) was subjected to silica gel column chromatography (630 g, 40 × 6.5 cm, $CHCl_3$−MeOH, 40:1−30:1−0:1) to afford seven subfractions, B1 to B7. Subfraction B3 (780.3 mg) was subjected to silica gel column chromatography (160 g, 80 × 2.7 cm, $CHCl_3$−EtOAc, 5:1−4:1−3:1, followed by MeOH) to obtain the racemic mixture **1** (281.9 mg) and a mixture of **2** and **4**. The latter was purified by semipreparative HPLC (CH_3CN−H_2O, 55:45) to obtain racemic mixtures **2** (t_R = 21.9 min, 71.5 mg) and **4** (t_R = 30.7 min, 74.1 mg). Purification by chiral semipreparative HPLC of racemic mixtures **1** (hexanes−IPA, 60:40), **2** (hexanes−IPA, 60:40), and **4** (hexanes−IPA, 65:35) afforded (+)-**1** (t_R = 6.2 min, 79.9 mg), (−)-**1** (t_R = 12.4 min, 78.3 mg), (+)-**2** (t_R = 6.6 min, 27.0 mg), (−)-**2** (t_R = 12.9 min, 28.8 mg), (+)-**4** (t_R = 7.4 min, 19.2 mg), and (−)-**4** (t_R = 24.5 min, 16.7 mg), respectively. Fraction C (2.9 g) was subjected to silica gel column chromatography (600 g, 39 × 6.5 cm, $CHCl_3$−EtOAc, 4:1−3:1, followed by MeOH) to afford racemic mixture **3** (400.2 mg). Part of the racemic mixture **3** (200.0 mg) was purified by chiral semipreparative HPLC (hexane−IPA, 60:40) to afford (+)-**3** (t_R = 7.7 min, 81.0 mg) and (−)-**3** (t_R = 15.6 min, 79.4 mg). Fraction D (618 mg) was submitted to silica gel column chromatography (120 g, 75 × 2.3 cm, $CHCl_3$−EtOAc, 4:1−3:1, then MeOH) followed by semipreparative HPLC (MeOH−H_2O, 80:20) to afford racemic mixture **5** (t_R = 31.7 min, 8.4 mg).

*(+)-Balsacone J [(+)-**1**]:* yellow, amorphous powder; $[\alpha]^{22}_D$ +8.6 (*c* 2.5, acetone); UV (MeOH) λ_{max} (log ε) 205 (4.60), 226 (4.43), 264 (4.22), 293 (4.15), 330 (3.67) nm; ECD (1.9 × 10^{-3} M, MeOH) $\Delta\varepsilon_{226}$ = −1.62, $\Delta\varepsilon_{239}$ = +1.12, $\Delta\varepsilon_{260}$ = −1.04, $\Delta\varepsilon_{287}$ = +2.00; IR (film) ν_{max} 3352, 3027, 2925, 1703, 1612, 1513, 1450, 1367, 1264, 1225, 1171, 1149, 1091, 1028, 967, 926, 833, 744, 713, 628, 571, 540, 522 cm^{-1}; for ^1H and ^{13}C NMR spectroscopic data, see Tables 1 and 2; APCI(+)MS *m*/*z* 523 $[M + H]^+$ (100), 271 (41), 133 (21); HRESIMS *m*/*z* 545.1945 $[M + Na]^+$ (calcd for $C_{33}H_{30}O_6Na$, 545.1935).

*(−)-Balsacone J [(−)-**1**]:* white crystals (IPA); mp decompose; $[\alpha]^{22}_D$ −7.9 (*c* 1.3, acetone); ECD (1.9 × 10^{-3} M, MeOH) $\Delta\varepsilon_{227}$ = +2.62, $\Delta\varepsilon_{240}$ = −1.42, $\Delta\varepsilon_{259}$ = +1.66, $\Delta\varepsilon_{286}$ = −2.46; UV, IR, ^1H and ^{13}C NMR, APCIMS, and ESIMS data were the same as for (+)-**1**.

*(+)-Iryantherin-D [(+)-**2**]:* yellow, amorphous powder; $[\alpha]^{25}_D$ +3.7 (*c* 0.22, acetone); UV (MeOH) λ_{max} (log ε) 202 (4.52), 225 (4.31), 264 (4.19), 285 (4.09), 292 (4.09), 330 (3.53) nm; ECD (1.8 × 10^{-3}

DOI: 10.1021/acs.jnatprod.5b00155
J. Nat. Prod. 2015, 78, 1147−1153

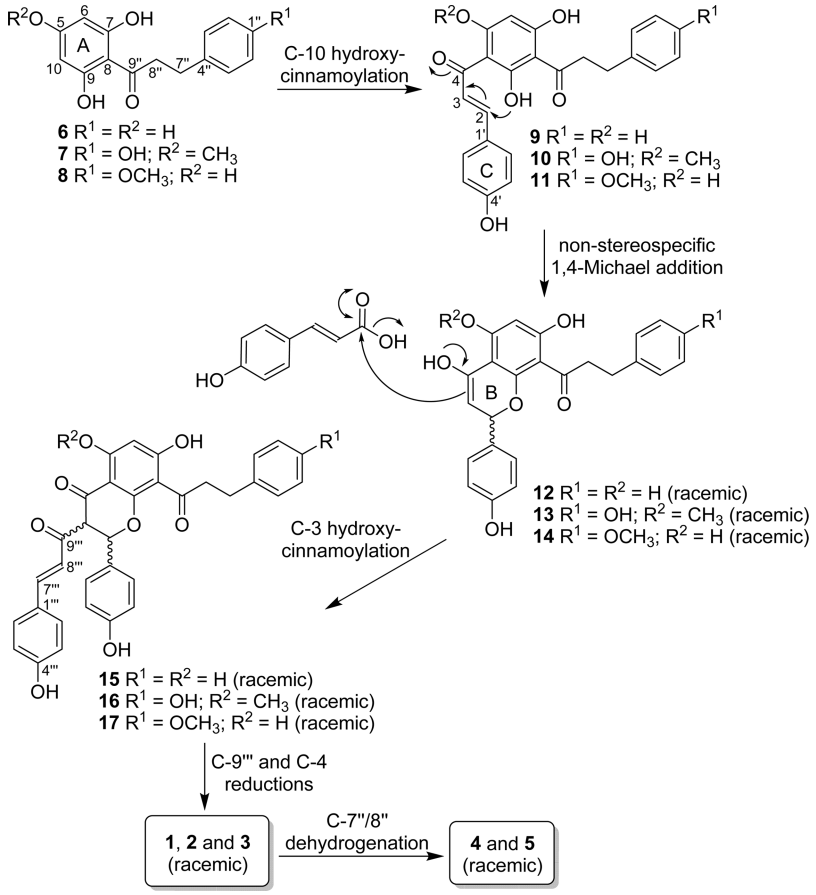

Figure 4. Proposed biosynthetic pathway for isolates **1**−**5**.

Table 3. In Vitro Antibacterial Activity of Compounds 1−5 against *S. aureus* (ATCC 25923)

compound	IC_{50}[a] (μM)
(−)-**1**	1.27 ± 0.07[b]
(+)-**1**	1.79 ± 0.09
(−)-**2**	2.27 ± 0.04[b]
(+)-**2**	4.3 ± 0.3
(−)-**3**	3.6 ± 0.7[b]
(+)-**3**	6 ± 1
(−)-**4**	0.61 ± 0.02[b]
(+)-**4**	2.27 ± 0.04
(±)-**5**	1.9 ± 0.2
chloramphenicol	0.43 ± 0.05
gentamycin	0.010 ± 0.002

[a]Concentration inhibiting 50% of bacterial growth after 24 h. [b]Significantly different from corresponding (+)-enantiomer using Wilcoxon signed-rank test ($p < 0.05$).

M, MeOH) $\Delta\varepsilon_{226}$ = −2.40, $\Delta\varepsilon_{237}$ = +1.55, $\Delta\varepsilon_{261}$ = −1.29, $\Delta\varepsilon_{287}$ = +2.18; IR ν_{max} 3356, 3027, 2927, 2837, 1889, 1700, 1611, 1512, 1448, 1425, 1368, 1236, 1176, 1150, 1106, 1090, 1035, 967, 926, 832, 685 cm^{-1}; for ^1H and ^{13}C NMR spectroscopic data, see Tables 1 and 2; APCI(+)MS *m/z* 553 $[M + H]^+$ (100), 301 (41), 133 (10); HRESIMS *m/z* 575.2034 $[M + Na]^+$ (calcd for $C_{34}H_{32}O_7Na$, 575.2040).

*(−)-Iryantherin-D [(−)-**2**]:* yellow, amorphous powder; $[\alpha]^{23}_D$ −2.4 (*c* 0.3, acetone); ECD (1.8 × 10^{-3} M, MeOH) $\Delta\varepsilon_{224}$ = +3.46, $\Delta\varepsilon_{239}$ = −1.64, $\Delta\varepsilon_{261}$ = +1.27, $\Delta\varepsilon_{285}$ = −2.16; UV, IR, ^1H and ^{13}C NMR, APCIMS, and HRESIMS data were the same as for (+)-**2**.

*(+)-Balsacone K [(+)-**3**]:* yellow, amorphous powder; $[\alpha]^{26}_D$ +1.2 (*c* 0.84, acetone); UV (MeOH) λ_{max} (log ε) 205 (4.77), 225 (4.65), 271 (4.51), 285 (4.46), 330 (3.79); ECD (1.3 × 10^{-3} M, MeOH) $\Delta\varepsilon_{225}$ = −1.46, $\Delta\varepsilon_{239}$ = +1.61, $\Delta\varepsilon_{259}$ = −0.57, $\Delta\varepsilon_{285}$ = +1.52; IR ν_{max} 3391, 3025, 2919, 1887, 1700, 1620, 1589, 1515, 1444, 1370, 1220, 1172, 1144, 1120, 968, 833, 702, 624, 603, 567 cm^{-1}; for ^1H and ^{13}C NMR spectroscopic data, see Tables 1 and 2; APCI(+)MS *m/z* 553 $[M + H]^+$ (100), 301 (74); HRESIMS *m/z* 575.2042 $[M + Na]^+$ (calcd for $C_{34}H_{32}O_7Na$, 575.2040).

*(−)-Balsacone K [(−)-**3**]:* yellow, amorphous powder; $[\alpha]^{25}_D$ −1.0 (*c* 2.5, acetone); ECD (1.0 × 10^{-3} M, MeOH) $\Delta\varepsilon_{226}$ = +2.82, $\Delta\varepsilon_{239}$ = −2.34, $\Delta\varepsilon_{260}$ = +1.04, $\Delta\varepsilon_{285}$ = −2.21; UV, IR, ^1H and ^{13}C NMR, APCIMS, and HRESIMS data were the same as for (+)-**3**.

*(+)-Balsacone L [(+)-**4**]:* yellow, amorphous powder; $[\alpha]^{22}_D$ +50.4 (*c* 1.0, acetone); UV (MeOH) λ_{max} (log ε) 204 (4.65), 262 (4.32), 310 (4.24), 349 (4.11) nm; ECD (1.9 × 10^{-3} M, MeOH) $\Delta\varepsilon_{224}$ = −1.66, $\Delta\varepsilon_{233}$ = +0.46, $\Delta\varepsilon_{258}$ = −1.71, $\Delta\varepsilon_{286}$ = +0.80; IR ν_{max} 3375, 2921, 1699, 1624, 1547, 1512, 1448, 1419, 1350, 1232, 1171, 1156, 1089, 1041, 969, 834, 777, 745, 688, 620, 576, cm^{-1}; for ^1H and ^{13}C NMR spectroscopic data, see Tables 1 and 2; APCI(+)MS *m/z* 553 $[M + H]^+$ (100), 301 (41), 133 (11); HRESIMS *m/z* 543.1781 $[M + Na]^+$ (calcd for $C_{33}H_{28}O_6Na$, 543.1778).

*(−)-Balsacone L [(−)-**4**]:* yellow, amorphous powder; $[\alpha]^{24}_D$ −54.7 (*c* 0.15, acetone); ECD (1.9 × 10^{-3} M, MeOH) $\Delta\varepsilon_{224}$ = +1.28, $\Delta\varepsilon_{233}$ = −0.32, $\Delta\varepsilon_{260}$ = +1.71, $\Delta\varepsilon_{286}$ = −0.55; UV, IR, ^1H and ^{13}C NMR, APCIMS, and HRESIMS data were the same as for (+)-**4**.

*Balsacone M (**5**):* yellow, amorphous powder; UV (MeOH) λ_{max} (log ε) 204 (4.78), 259 (4.32), 371 (4.47) nm; IR ν_{max} 3356, 3027, 2928, 1620, 1545, 1512, 1443, 1352, 1290, 1230, 1169, 1148, 1120, 1049, 994, 968, 832; for ^1H and ^{13}C NMR spectroscopic data, see Tables 1 and 2; APCI (+) MS *m/z* 551 $[M + H]^+$ (100), 299 (14); HRESIMS *m/z* 573.1871 $[M + Na]^+$ (calcd for $C_{34}H_{30}O_7Na$, 573.1884).

DOI: 10.1021/acs.jnatprod.5b00155
J. Nat. Prod. 2015, 78, 1147−1153

X-ray Crystal Structure Analysis of (−)-1. Diffraction intensity data were collected by a Bruker Smart diffractometer equipped with an APEX II CCD detector employing graphite-monochromated Cu Kα radiation (λ = 1.541 78 Å) at 100 K. The structure was solved by direct methods with SHELXS-97 and refined with full-matrix least-squares calculations on F^2 using SHELX-97.[15] Crystallographic data for compound (−)-**1** have been deposited at the Cambridge Crystallographic Data Center (deposition no. CCDC 1024869). Copies of these data can be obtained free of charge via www.ccdc.cam.ac.uk/conts/retrieving.html or from the Cambridge Crystallographic Data Center, 12 Union Road, Cambridge CB21EZ, UK (fax: +44 1223 336033; e-mail: deposit@ccdc.cam.ac.uk).

Conformational Analysis, Geometrical Optimization, and ECD Calculation for (2*S*,3*S*)-1, (2*S*,3*S*)-2, (2*S*,3*S*)-3, and (2*S*,3*S*)-4. Monte Carlo conformational searching was carried out by molecular mechanics using the MMFF94 force field with the Spartan '10 V1.1.0 program (Wavefunction Inc.). An energy cutoff of 5 kcal/mol was chosen in order to select a wide distribution of conformers. Selected conformers were submitted to single-point energy calculation using DFT with the B3LYP functional and 6-31G(d) basis set in the Gaussian 09 software.[16] Geometry optimization followed by thermodynamic properties calculation of the structures was carried out on conformers within an energy cutoff of 1 kcal/mol. Energy and rotational strength calculations using the TDDFT method with the B3LYP functional and 6-311G(2d,2p) basis set considering 40 electronic transitions were conducted for the optimized conformers. Effects of solvent (MeOH) were taken into account using the IEF-PCM model. ECD spectra were simulated from these data by overlapping Gaussian functions for each transition according to

$$\Delta\varepsilon(E) = \frac{1}{2.297 \times 10^{-39}} \frac{1}{\sqrt{2\pi\sigma}} \sum_{i}^{A} \Delta E_i R_i e^{-[(E-\Delta E_i)/(2\sigma)]^2}$$

where σ is the width of the band at $1/e$ height (set at 0.10−0.15) and ΔE_i and R_i are the excitation energies and rotatory strengths for transition i, respectively.

Bacterial Growth Inhibition Assay. Antibacterial activity against *S. aureus* (strain ATCC 25923) was evaluated using the microdilution method with modifications as previously reported.[12,17] Gentamycin and chloramphenicol were used as positive controls. The results are expressed as the concentration inhibiting 50% of bacterial growth (IC_{50}). The IC_{50} values were evaluated after 24 h of growth.

Cytotoxicity Assay. Cytotoxicity was evaluated against the human fibroblast cell line (WS1) using the resazurin reduction test as previously reported.[18,19] Cytotoxicity was expressed as the concentration inhibiting 50% of cell growth (IC_{50}). Etoposide was used as a positive control.

■ ASSOCIATED CONTENT

Ⓢ Supporting Information

^{1}H and ^{13}C NMR spectra for compounds **1**−**5** and X-ray crystallographic data for compound (-)-**1**. The Supporting Information is available free of charge on the ACS Publications website at DOI: 10.1021/acs.jnatprod.5b00155.

■ AUTHOR INFORMATION

Corresponding Author

*Tel: +1 (418) 545-5011, ext 5081. E-mail: andre.pichette@uqac.ca.

Notes

The authors declare no competing financial interest.

■ ACKNOWLEDGMENTS

This project was supported by the Natural Sciences and Engineering Research Council of Canada (NSERC) and by the Fonds de Recherche Nature et Technologies (Ph.D. fellowships to F.S.). We acknowledge the "Chaire de Recherche sur les Agents Anticancéreux d'Origine Naturelle" for funding. This research has been enabled by the use of computing resources provided by WestGrid and Compute/Calcul Canada. The authors would like to thank F. Otis and N. Voyer from PROTEO and Université Laval for their help in recording circular dichroism spectra as well as C. Dusseault for her technical assistance in the evaluation of antibacterial and cytotoxic activities.

■ REFERENCES

(1) Walsh, C. T.; Wencewicz, T. A. *J. Antibiot.* **2014**, *67*, 7.
(2) Coates, A. R. M.; Halls, G.; Hu, Y. *Br. J. Pharmacol.* **2011**, *163*, 184.
(3) Taylor, P. W. *Int. J. Antimicrob. Agents* **2013**, *42*, 195.
(4) Uprety, Y.; Asselin, H.; Dhakal, A.; Julien, N. *J. Ethnobiol. Ethnomed.* **2012**, *8*, 7.
(5) Koné, W. M.; Atindehou, K. K.; Terreaux, C.; Hostettmann, K.; Traoré, D.; Dosso, M. *J. Ethnopharmacol.* **2004**, *93*, 43.
(6) Bonjar, S. *J. Ethnopharmacol.* **2004**, *94*, 301.
(7) Omar, S.; Lemonnier, B.; Jones, N.; Ficker, C.; Smith, M. L.; Neema, C.; Towers, G. H. N.; Goel, K.; Arnason, J. T. *J. Ethnopharmacol.* **2000**, *73*, 161.
(8) Navarro, V.; Villarreal, M. L.; Rojas, G.; Lozoya, X. *J. Ethnopharmacol.* **1996**, *53*, 143.
(9) Saleem, M.; Nazir, M.; Ali, M. S.; Hussain, H.; Lee, Y. S.; Riaz, N.; Jabbar, A. *Nat. Prod. Rep.* **2010**, *27*, 238.
(10) Gibbons, S. *Nat. Prod. Rep.* **2004**, *21*, 263.
(11) Simard, F.; Legault, J.; Lavoie, S.; Pichette, A. *Phytochemistry* **2014**, *100*, 141.
(12) Lavoie, S.; Legault, J.; Simard, F.; Chiasson, É.; Pichette, A. *Tetrahedron Lett.* **2013**, *54*, 1631.
(13) Pelter, A.; Stainton, P.; Barber, M. *J. Heterocycl. Chem.* **1965**, *2*, 262.
(14) Conserva, L. M.; Yoshida, M.; Gottlieb, O. R.; Martinez V, J. C.; Gottlieb, H. E. *Phytochemistry* **1990**, *29*, 3911.
(15) Sheldrick, G. M. *Acta Crystallogr. Sect. A: Found. Crystallogr.* **2008**, *64*, 112.
(16) Frisch, M. J.; Trucks, G. W.; Schlegel, H. B.; Scuseria, G. E.; Robb, M. A.; Cheeseman, J. R.; Scalmani, G.; Barone, V.; Mennucci, B.; Petersson, G. A.; Nakatsuji, H.; Caricato, M.; X. Li, H. P. H.; Izmaylov, A. F.; Bloino, J.; Zheng, G.; Sonnenberg, J. L.; Hada, M.; Ehara, M.; Toyota, K.; Fukuda, R.; Hasegawa, J.; Ishida, M.; Nakajima, T.; Honda, Y.; Kitao, O.; Nakai, H.; Vreven, T.; J. A. Montgomery, J.; Peralta, J. E.; Ogliaro, F.; Bearpark, M.; Heyd, J. J.; Brothers, E.; Kudin, K. N.; Staroverov, V. N.; Keith, T.; Kobayashi, R.; Normand, J.; Raghavachari, K.; Rendell, A.; Burant, J. C.; Iyengar, S. S.; Tomasi, J.; Cossi, M.; Rega, N.; Millam, J. M.; Klene, M.; Knox, J. E.; Cross, J. B.; Bakken, V.; Adamo, C.; Jaramillo, J.; Gomperts, R.; Stratmann, R. E.; Yazyev, O.; Austin, A. J.; Cammi, R.; Pomelli, C.; Ochterski, J. W.; Martin, R. L.; Morokuma, K.; Zakrzewski, V. G.; Voth, G. A.; Salvador, P.; Dannenberg, J. J.; Dapprich, S.; Daniels, A. D.; Farkas, O.; Foresman, J. B.; Ortiz, J. V.; Cioslowski, J.; Fox, D. J. *Gaussian 09*; Gaussian Inc., 2010.
(17) Banfi, E.; Scialino, G.; Monti-Bragadin, C. *J. Antimicrob. Chemother.* **2003**, *52*, 796.
(18) O'Brien, J.; Wilson, I.; Orton, T.; Pognan, F. *Eur. J. Biochem.* **2000**, *267*, 5421.
(19) Bellila, A.; Tremblay, C.; Pichette, A.; Marzouk, B.; Mshvildadze, V.; Lavoie, S.; Legault, J. *Phytochemistry* **2011**, *72*, 2031.

DOI: 10.1021/acs.jnatprod.5b00155
J. Nat. Prod. 2015, 78, 1147−1153